This article was downloaded by:
On: *25 January 2011*
Access details: *Access Details: Free Access*
Publisher *Taylor & Francis*
Informa Ltd Registered in England and Wales Registered Number: 1072954 Registered office: Mortimer House, 37-41 Mortimer Street, London W1T 3JH, UK

Liquid Crystals
Publication details, including instructions for authors and subscription information:
http://www.informaworld.com/smpp/title~content=t713926090

Synthesis, photo-reaction and photo-induced liquid crystal alignment of soluble polyimide with pendant cinnamate group

Hee-Tak Kim[a]; Jong-Woo Lee[a]; Shi-Joon Sung[a]; Jung-Ki Park[a]
[a] Department of Chemical Engineering, Korea Advanced Institute of Science and Technology, 371-1 Yusung-gu, Kusung-dong, Daejon 305-701, Korea,

Online publication date: 06 August 2010

To cite this Article Kim, Hee-Tak , Lee, Jong-Woo , Sung, Shi-Joon and Park, Jung-Ki(2000) 'Synthesis, photo-reaction and photo-induced liquid crystal alignment of soluble polyimide with pendant cinnamate group', Liquid Crystals, 27: 10, 1343 — 1356
To link to this Article: DOI: 10.1080/026782900423403
URL: http://dx.doi.org/10.1080/026782900423403

PLEASE SCROLL DOWN FOR ARTICLE

Full terms and conditions of use: http://www.informaworld.com/terms-and-conditions-of-access.pdf

This article may be used for research, teaching and private study purposes. Any substantial or systematic reproduction, re-distribution, re-selling, loan or sub-licensing, systematic supply or distribution in any form to anyone is expressly forbidden.

The publisher does not give any warranty express or implied or make any representation that the contents will be complete or accurate or up to date. The accuracy of any instructions, formulae and drug doses should be independently verified with primary sources. The publisher shall not be liable for any loss, actions, claims, proceedings, demand or costs or damages whatsoever or howsoever caused arising directly or indirectly in connection with or arising out of the use of this material.

LIQUID CRYSTALS, 2000, VOL. 27, NO. 10, 1343–1356

Synthesis, photo-reaction and photo-induced liquid crystal alignment of soluble polyimide with pendant cinnamate group

HEE-TAK KIM, JONG-WOO LEE, SHI-JOON SUNG and JUNG-KI PARK*

Department of Chemical Engineering,
Korea Advanced Institute of Science and Technology, 371-1 Yusung-gu,
Kusung-dong, Daejon 305-701, Korea

(*Received 20 September 1999; accepted 27 April 2000*)

In this paper, the synthesis, photo-reaction and photo-induced liquid crystal alignment of a polyimide with a pendant cinnamate group are reported. The polyimide was synthesized by the thermal imidization of the polyamic acid derived from 4,4′-(hexafluoro-isopropylidene)-diphthalic anhydride and hydroxydiaminopropane, followed by the attachment of the cinnamate group to the main chain polyimide. The surface of thin layers of the polyimide was found to be preferentially occupied by the pendant cinnamate groups, and liquid crystal alignment on the polyimide thin film exposed to polarized UV was independent of the cinnamate content. The thermal stability of the photo-induced liquid crystal alignment was enhanced with decrease in the cinnamate content. This could be attributed to the strong interchain interaction of the polyimide chains which prevents thermal randomization of the photo-product of the pendant cinnamates. The dependences of the photo-reaction temperature and the annealing temperature of the alignment layer on the azimuthal anchoring energy of the photo-aligned liquid crystal suggest that the local stress developed during the UV irradiation profoundly influences the thermal stability of the liquid crystal alignment.

Downloaded At: 18:24 25 January 2011

1. Introduction

In recent years, a considerable amount of research has been directed towards photo-induced liquid crystal (LC) alignment [1–22]. This technique uses the exposure of a polymer film to polarized UV for developing a structural anisotropy on its surface. As a result of the anisotropic interaction between the LC and the film surface, unidirectional alignment of the LC is induced. It has been reported that LC alignment occurs with films having a *cis-trans*-conformational transition of a chromophore [1–3], photo-crosslinking [4–10], and photo-dissociation of the polymer [11, 12].

A thin film of poly(vinyl cinnamate) (PVCi), one of the representative photo-crosslinkable photoresists has attracted special attention owing to the high photo-reactivity of the cinnamate group which provides a photo-active surface for achieving the photo-control of in-plane alignment of the LC with polarized UV irradiation [4, 7, 8, 14, 15, 21]. However, additional requirements must be satisfied before the polymer can demonstrate its potential as an actual device material. Some of these include good thermal stability of the photo-induced LC alignment which is closely associated with the thermal stability of the material. In that sense, an insufficient thermal stability of the photo-induced LC alignment on the PVCi layer is a major hindrance to further progress in developing liquid crystal displays (LCDs) [5]. The disruption of the LC alignment is believed to be a result of a significant thermal relaxation of the PVCi chain, which causes the randomization of the anisotropic distribution of a photo-product [5].

It is thus necessary to develop a new type of polymeric alignment layer which exhibits a significantly hindered thermal relaxation of the chains. In this work, a new soluble cinnamate-grafted polyimide based on 4,4′-(hexafluoro-isopropylidene)diphthalic anhydride and hydroxydiaminopropane was prepared and used as an alignment layer for the photo-induced LC alignment. The introduction of the imide segment in the main chain was aimed at providing thermal stability of the LC alignment derived from the photo-reaction of the pendant cinnamate groups. The structural changes of the polymers upon the polarized UV irradiation and the consequent photo-induced LC alignment behaviour were investigated with varying cinnamate content in order to understand the mechanism of the photo-induced LC alignment on the thin layer of the polyimides with pendant cinnamate groups. The thermal stability of the photo-induced LC alignment was also evaluated.

*Author for correspondence, e-mail: pjk@mail.kaist.ac.kr

Liquid Crystals ISSN 0267-8292 print/ISSN 1366-5855 online © 2000 Taylor & Francis Ltd
http://www.tandf.co.uk/journals

Downloaded At: 18:24 25 January 2011

2. Experimental

2.1. *Materials*

4,4′-(Hexafluoro-isopropylidene)diphthalic anhydride (6-FDA), 2-hydroxy-1,3-diaminopropan e (HDAP), and cinnamoyl chloride were reagent grade from Aldrich and used as supplied. *m*-Cresol, the solvent for the synthesis of the polyimide and pyridine, and the solvent for the reaction grafting the cinnamoyl chloride to the polyimide, were purified by vacuum distillation and stored under nitrogen. All other reagents and solvents (reagent grade) were used as received without further purification.

2.2. *Synthesis of the soluble polyimide derived from 6-FDA and HDAP*

To a 20 ml glass reactor were added 0.17 g of HDAP and 5 ml of *m*-cresol. The solution was stirred for 1 h under nitrogen, and then the equimolar amount of 6-FDA (0.83 g) was added to the reactor. After a pink viscous solution had been obtained, the reaction temperature was elevated to 180°C and a catalytic amount of isoquinoline was added to the mixture to accelerate the conversion of the amic acid group to the imide group. The reaction was allowed to proceed for 12 h under nitrogen. After completion of the imidization reaction, the resulting solution was poured into cold methanol to precipitate the polyimide. The filter cake was washed several times with methanol and ethyl ether and dried under vacuum at 100°C for 12 h.

2.3. *Grafting of the cinnamate group to the 6-FDA-HDAP polyimide*

The polyimide (0.25 g) was dissolved in 5 ml of pyridine and an equivalent amount of cinnamoyl chloride was added. These procedures were executed in a glove box under argon to prevent water contamination of the reactants. The grafting reaction took 3 h at room temperature, after which the mixture was poured into cold methanol to precipitate the cinnamate-grafted polyimide. The unreacted cinnamoyl chloride was removed with methanol. The precipitate was purified by further washing with methanol and drying under vacuum at 80°C for 12 h.

2.4. *Structural and thermal characterization of the polyimides*

The structures of the polyimides were characterized using proton nuclear magnetic resonance spectroscopy (^{1}H NMR; Bruker-AMX-500 NMR spectrometer). The solvent used for sample preparation was DMSO-d_6. Tetramethylsilane was used as a reference for peak assignments.

Thermal analysis was also carried out under nitrogen by differential scanning calorimetry (DSC) (DuPont Thermal Analyst 2000 model).

2.5. *Spectroscopic measurements*

UV spectra were recorded with a Hewlett Packard 8452A spectrometer. All measurements were done with quartz slides as substrate. The uncoated part of the slide was used as a reference.

FTIR spectra were acquired on a Bomem 102 model fourier transform spectrometer at a resolution of 4 cm^{-1}. A minimum of 40 scans were signal-averaged and the spectra stored on a magnetic disc system for further analysis.

X-ray photo-electron spectroscopy (XPS) analysis of the polyimide layers was carried out using a monochromatic microspot X-ray beam originating from a MgK_α source (1253.6 eV photons) with a spot diameter of about 600 μm from a Surface Analysis System SPECS LHS10 spectrometer. The X-ray source was run at a reduced power of 120 W (12 kV and 10 mA). Throughout the measurement, the pressure in the analysis chamber was maintained at 10^{-8} mbar or lower. To compensate for the surface charging effect, all binding energies were calibrated with reference to the neutral carbon C1s line taken at 284.6 eV.

2.6. *Film preparation*

A 1 wt% *N*-methylpyrrolidone (NMP) solution of the polyimide with a pendant cinnamate group was spin-coated onto a glass substrate at 1800 rpm and the cast was baked at 180°C to remove any residual NMP. The thickness of the layer was adjusted to be about 50 nm. The photo-reaction of the thin layer of the polymer was carried out by irradiating the layer with polarized UV at normal incidence. The polarized UV light (250 ~ 340 nm) for the irradiation was obtained by passing the light from a 300 W high mercury arc (Oriel) through a UV linear dichroic polarizer (27 320, Oriel) and a UV filter (51 650, Oriel). The intensity of the irradiating UV measured by a UV detector (UIT-150, Ushio) was 5 mW cm^{-2}.

2.7. *Fabrication of the homogeneously aligned LC cell*

A homogeneously aligned LC cell was constructed by sandwiching the nematic LC (E7) between a pair of glass substrates covered with a thin layer of the polyimide, and sealed with epoxy resin adhesive. The thickness of the LC layer was adjusted by spherical spacers of 8 μm diameter. E7 liquid crystal was injected into the cell by capillary action at 65°C in the isotropic phase, and the cell was gradually cooled to room temperature. The texture of the liquid crystal in the cell between crossed polarizers was investigated using a Nikon OPTOPHOTO2-POL polarizing optical microscope.

Downloaded At: 18:24 25 January 2011

2.8. *Determination of alignment direction, azimuthal anchoring energy, order parameter and pretilt angle of the photo-aligned nematic LC*

The director of the nematic LC in the homogeneously aligned LC cell was determined from the dichroic absorption of a dichroic dye (disperse blue 14) dissolved in the LC layer in the cell. A small amount of the dichroic dye (1 wt %) was dissolved in the E7 liquid crystal. The dichroic dye shows a strong absorption at 656 nm and from the angular dependency of this absorption in the polarized UV spectra of the LC, the distribution of the LC director can be obtained. The dichroic ratio (R) for the anisotropic absorption of the dichroic dye was also determined from the polarized UV spectra of the LC cells. The order parameter of the liquid crystal (S) can also be obtained from the dichroic ratio for the anisotropic absorption of the dichroic dye using the relation: $S = (R - 1)/(R + 2)$.

The azimuthal anchoring energy of the LC on the alignment layer was determined by measuring the width of a disclination wall called a Neel wall which is observed in homogeneously aligned LC cells. The width of the Neel wall, w, is defined as the distance between two black brushes where the director is rotated from 45° to 135° with respect to the director in a uniformly aligned region. The azimuthal anchoring energy is then calculated using the following formula.

$$E_{\varphi} = 2dK_1/w^2 \qquad (1)$$

where K_1 and d represent the splay elastic constant and the thickness of the LC layer, respectively. A detailed description of the determination of the azimuthal anchoring energy by observing Neel walls can be found elsewhere [8, 23].

The pretilt angle of the nematic LC was measured by the crystal rotation method as described elsewhere [24, 25]. From the transmittance as a function of the incident angle of a He-Ne laser beam as the probing light passed through a cell set between two crossed polarizers, the value for the pretilt angle was determined.

3. Results and discussion

3.1. *Synthesis of the soluble polyimide with a pendant cinnamate group*

The synthesis of the soluble polyimide with a pendant cinnamate group was performed as summarized in figure 1. After addition of 6-FDA to the *m*-cresol solution of HDAP, the colour of the solution changed from yellow to pink and this was accompanied by an increase in viscosity, indicative of the formation of the polyamic acid. On heating with a catalytic amount of isoquinoline at 180°C, the reaction mixture became dark and remained homogeneous, producing no precipitate after completion

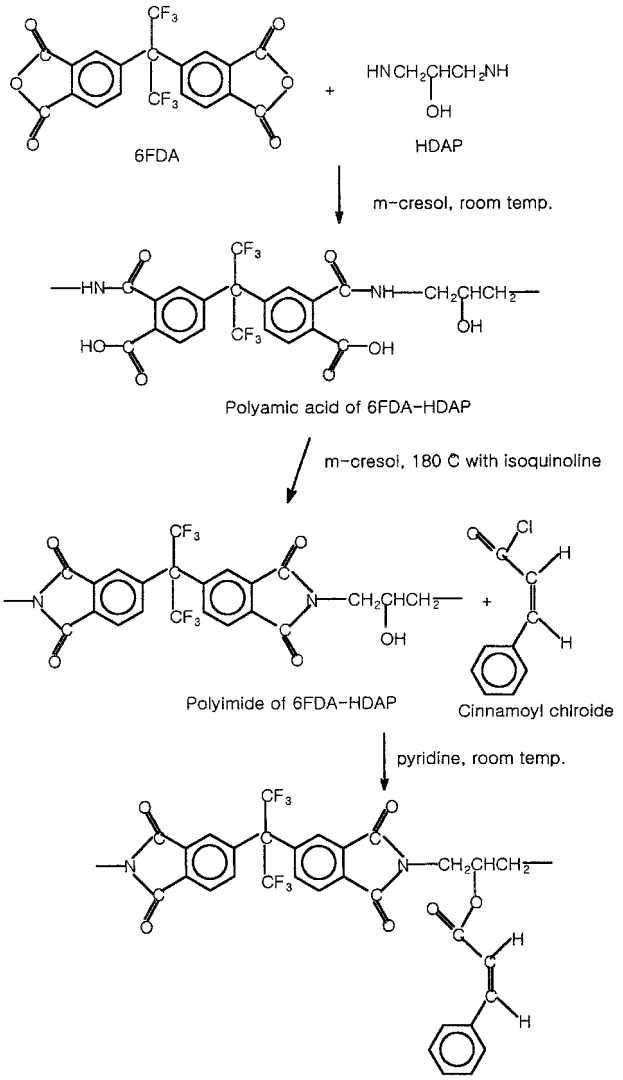

Figure 1. Synthetic scheme for the polyimides with pendant cinnamate groups.

of the reaction. The polyimide derived from 6-FDA and HDAP was obtained as a white powder on pouring the solution into an excess of methanol. The trace of isoquinoline was removed by washing with methanol. The yield was 85%. The mass averaged molecular mass and polydispersity index of the polyimide were 63 000 and 2.8, respectively.

The level of cinnamate substitution was controlled by adjusting the amount of cinnamoyl chloride used. The product was precipitated by pouring the solution into an excess of methanol. The yield was in the range 60–78% depending on the degree of cinnamate substitution.

For brevity, the polyimide with the pendant cinnamate group will be designated in this paper as PI-CIN*n*, where *n* indicates the mol % of the monomeric unit with the pendant cinnamate group.

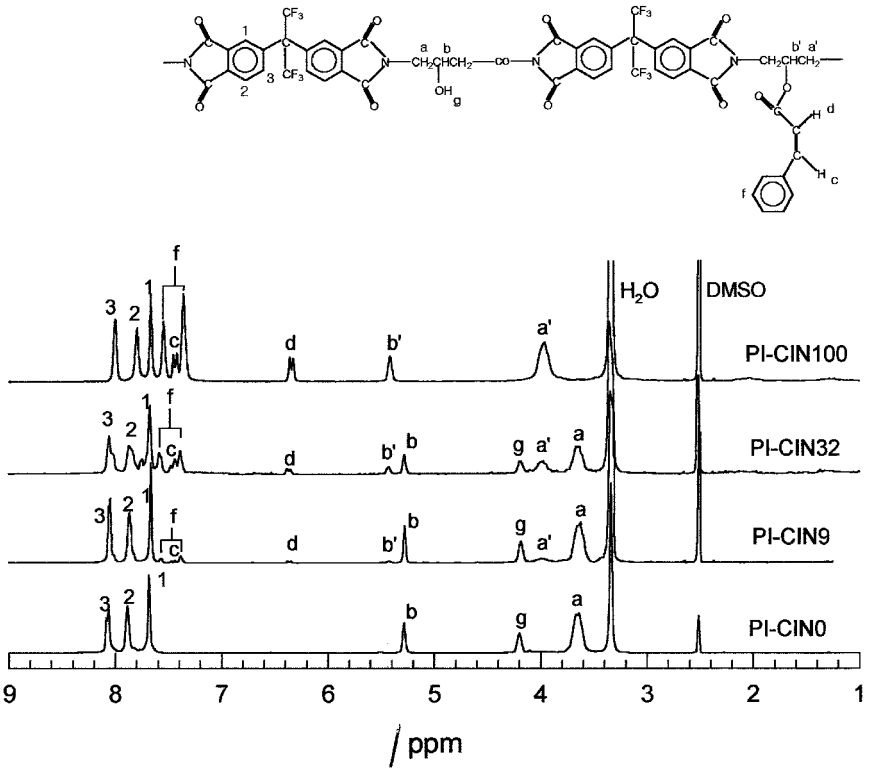

Figure 2. ^{1}H NMR spectra for the PI-CINs.

Downloaded At: 18:24 25 January 2011

3.2. *Structural and thermal characterization of the PI-CINs*

The ^{1}H NMR spectra of some PI-CINs are shown in figure 2. In the case of incomplete conversion of the amic acid group, the hydroxy proton from HDAP adjacent to the amic acid unit was found at 4.09 ppm. This disappeared when the reaction temperature exceeded 150°C, and confirmed complete conversion of the amic acid group into the imide group. The chemical shift of the hydroxy proton adjacent to the imide segment was found at 4.18 ppm.

After attachment of the cinnamate group to the polyimide, chemical shifts of the methine and the methylene protons from 5.27 to 5.41 ppm and from 3.65 to 3.95 ppm, respectively, were observed. The chemical shifts for the protons in the 6-FDA unit with attachment of the cinnamate group were less than 0.1 ppm. The peaks in the range 7.35–7.44 ppm and the doublet at 6.33 ppm correspond to the protons in the cinnamate group. This assignment was based on the ^{1}H NMR spectra of pure PVCi [26]. From the relative peak area of the methine proton of the cinnamate-attached unit and that of the unattached unit, the cinnamate content in the polyimide was determined.

The glass transition temperatures of the PI-CINs with various cinnamate contents as determined by DSC are given in figure 3. With increase of the cinnamate content, the T_g varied from 240 to 183°C. The steric limitation

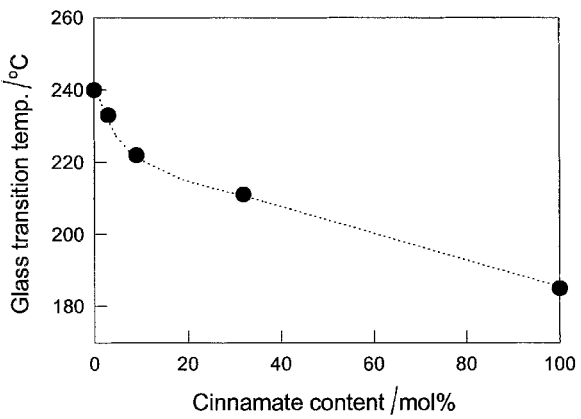

Figure 3. Glass transition temperatures of the PI-CINs as a function of cinnamate content.

in the ordering of the main chains and the free volume generated by the pendant cinnamate groups would contribute to the decrease in T_g with increasing cinnamate content. These polyimides are amorphous, as evidenced by the absence of a melting endotherm in the DSC thermograms.

3.3. *Spectroscopic characterization of the PI-CINs*

The UV spectra of PI-CINs with different cinnamate contents are compared in figure 4. The peak centred at 284 nm, of which the intensity increases with cinnamate content, corresponds to the absorption of the cinnamate

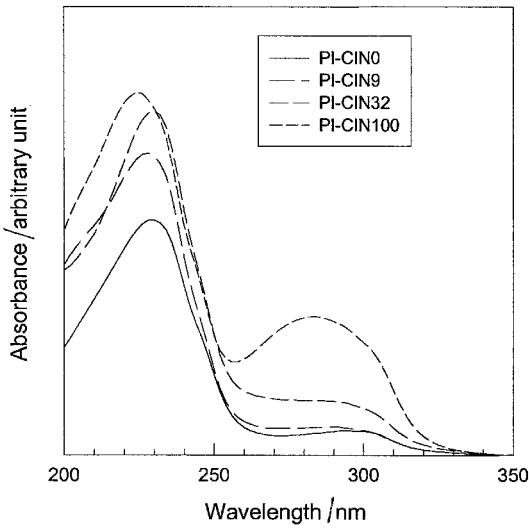

Figure 4. UV spectra for PI-CIN0, PI-CIN9, PI-CIN32 and PI-CIN100.

chromophore. The strong peak at about 228 nm and the broad band in the range 280–320 nm originate from the benzene rings and imide groups of the main chain [27]. It is interesting to note that for PI-CIN100, the strong absorption from the polyimide main chain appears at a somewhat shorter wavelength compared with those for PI-CIN0, PI-CIN9, and PI-CIN32. This indicates that, for PI-CIN100, the interaction between the imide segments is weaker than those for PI-CINs with a lower cinnamate content, due to the steric limitations imposed by the pendant cinnamate. When there is a strong interaction between the imide segments, conjugation involving the imide group is increased since rotation of the phenyl group results in an increased coplanarity with the imide group. The rotation into the planar conformation is favourable because electron delocalization is maximized by the π-orbital overlap in the more coplanar structure [28]. The lower energy state of the electrons in the imide segments due to the increased conjugation of the ordered imide segments consequently results in a red shift of the UV absorptions for PI-CINs with lower cinnamate contents.

Additional evidence for the difference in the intermolecular interactions between the main chains with a cinnamate content can be found from a comparison of the FTIR spectra of PI-CINs with different cinnamate contents. Figure 5 shows the FTIR spectra of PI-CIN0, PI-CIN9, and PI-CIN100 in the range 1650–1850 cm^{-1}. The symmetric C=O stretching and asymmetric C=O stretching peaks from the imide group are found at around 1780 and 1720 cm^{-1}, respectively [29–31]. For PI-CIN0 and PI-CIN9, the symmetric C=O stretching and asymmetric C=O stretching peaks were observed at lower wavenumbers than those for PI-CIN100. On account of the delocalization of the electrons in the ordered imide segments, the electron density of the C=O band decreases, resulting in the decrease in vibrational frequency of the C=O stretch.

3.4. *Surface structure of the PI-CIN thin layers*

Since liquid crystal alignment is mainly governed by the surface of the alignment layer, the surface structure of the thin layer of the PI-CINs is of critical importance. To obtain qualitative information about the surface structure, the contact angles of water and ethylene glycol were measured and the surface energy determined from these contact angles for the thin PI-CIN layers. As shown in table 1, profound differences in the contact angle and the surface energy are seen between PI-CIN0 and the PI-CINs with a pendant cinnamate group. These results imply that the pendant cinnamate group mainly determines the characteristics of the surface. However, the

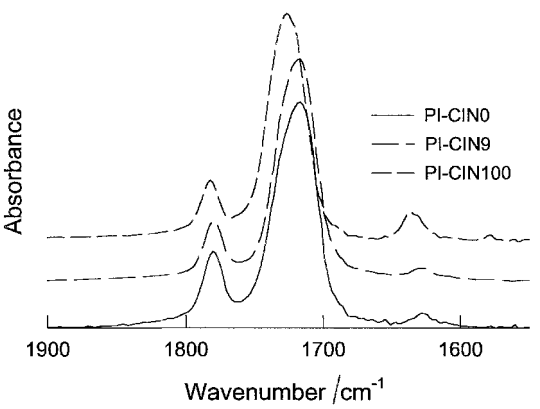

Figure 5. FTIR spectra in the range 1500–1900 cm^{-1} for PI-CIN0, PI-CIN9, and PI-CIN100.

Table 1. Water contact angle and surface energy[a] of polyimides with pendant cinnamate groups.

Sample	Water contact angle/°	Ethylene glycol contact angle/°	γ^d/(dispersion part) (dyne/cm)	γ^p/(polar part)	$\gamma^t/(\gamma^d + \gamma^p)$
PI-CIN0	37.9	40.2	2.6	60.2	62.8
PI-CIN9	66.0	46.1	16.3	19.0	35.3
PI-CIN32	68.9	46.5	15.4	19.1	34.5
PI-CIN100	73.7	46.8	24.7	10.0	34.7

[a] Calculated from the water and ethylene glycol contact angles using the equation: $1 + \cos\theta = 2[(\gamma_S^d\gamma_L^d)^{1/2} + (\gamma_S^p\gamma_L^p)^{1/2}]/\gamma_L^t$.

Downloaded At: 18:24 25 January 2011

contact angles for PI-CIN9, PI-CIN32, and PI-CIN100 were quite similar. Considering the relatively low surface energy for the PI-CINs in comparison with the surface energy for PI-CIN0, it is expected that this orientation of the pendant cinnamate group toward the surface is preferred to minimize the surface energy.

The spectroscopic investigation of the surface structure of thin PI-CIN layers was carried out by XPS analysis. Figure 6 shows the XPS spectra of PI-CIN9 and PI-CIN100 layers. The peaks corresponding to the elements F, O, N and C are clearly shown. Since fluorine and nitrogen are present only in the polyimide main chain, the relative contents of F and N atoms can be indicative of the population of the main chain. For a quantitative analysis, the area of each peak was divided by an atomic sensitivity factor, and the relative atomic content based on the carbon atom content was calculated. Table 2 lists the relative atomic contents for C, O, N, and F. Both PI-CIN9 and PI-CIN100 showed much lower N and F contents than those calculated from the molecular structure of the polyimides which represents the bulk composition. From the contact angle and XPS results, it can be reasonably concluded that the surface of the PI-CIN thin film is preferentially occupied by the pendant cinnamate groups.

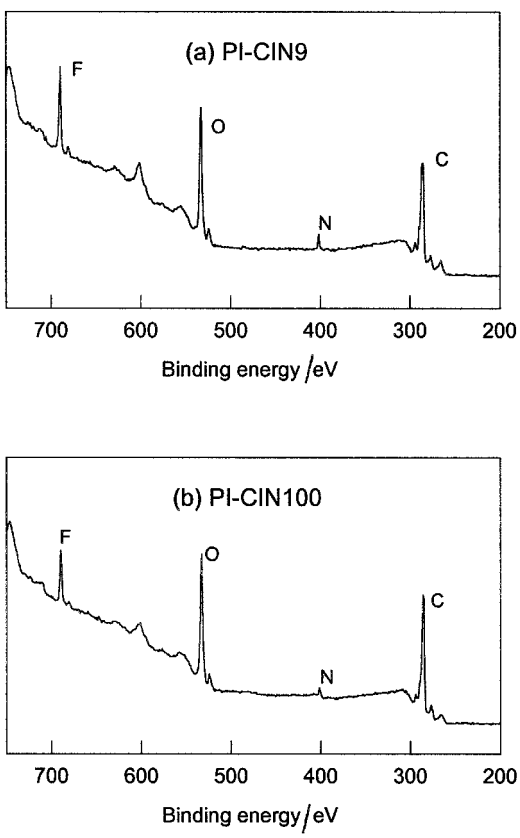

Figure 6. XPS spectra for (*a*) PI-CIN9 and (*b*) PI-CIN100.

Table 2. Relative content of atoms on the surface obtained from XPS analysis.

Sample	C1s	O1s	N1s	F1s
PI-CIN9	1 (1)	0.27 (0.23)	0.030 (0.09)	0.11 (0.26)
PI-CIN100	1 (1)	0.26 (0.23)	0.026 (0.065)	0.065 (0.194)

3.5. *Photo-reaction of the PI-CIN thin layers*

The photo-reaction of a cinnamate group in PVCi is generally characterized by *cis-trans*-photo-isomerization and photo-dimerization as shown below [32].

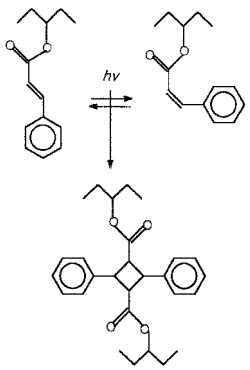

Egerton *et al.* [32] previously suggested that simultaneous progress of photo-isomerization and photo-dimerization occurs in solution as well as in a solid thin film of PVCi, but that isomerization plays only a minor role and does not seriously interfere with dimerization in a thin film. It was also proposed that the high extent of photo-dimerization in a solid film may be attributed to the ensemble of polymer bound cinnamoyl groups [33, 34]. For PI-CINs, besides photo-isomerization and photo-dimerization of the cinnamate group, photo-degradation of the polyimide is also expected to occur.

Figure 7 shows the changes in the UV spectra for the thin PI-CIN layers during irradiation with polarized UV (5 mW cm^{-2}). PI-CIN0 shows a slight decrease in the absorbances centred at 230 and 280 nm with irradiation time, indicating the occurrence of photo-degradation of the polyimide main chain. For PI-CIN9, a decrease in the absorbance at 284 nm with irradiation is observed. Moreover, the spectral curves obtained on progressive irradiation for longer than 20 min (> 6 J cm^{-2}) intersect at an isobestic point at 270 nm, as is generally observed for an exclusive *cis-trans*-isomerization [35, 36]. PI-CIN32 and PI-CIN100 reveal a significant decrease in the absorbance at 284 nm with irradiation as a result of photo-dimerization of the cinnamate groups, and show no isobestic point. The appearance of an isobestic point for PI-CIN9 after irradiation for 20 min, in contrast to the cases of PI-CIN32 and PI-CIN100, indicates that the photo-dimerization of PI-CIN9 was complete at a shorter irradiation time compared with PI-CIN32 and

Downloaded At: 18:24 25 January 2011

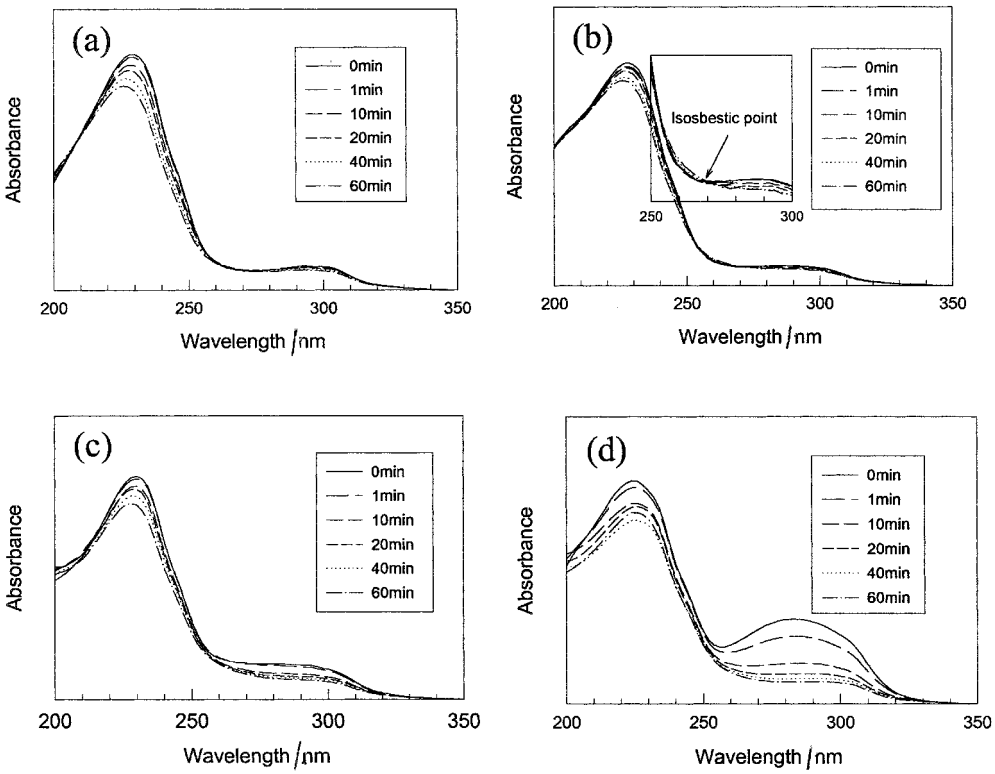

Figure 7. Change of UV spectra with p-UV irradiation for (*a*) PI-CIN0, (*b*) PI-CIN9, (*c*) PI-CIN32, (*d*) PI-CIN100.

Downloaded At: 18:24 25 January 2011

PI-CIN100. It is believed that, for PI-CIN9, pairs of cinnamate groups in proximity rapidly participates in dimerization, and the remaining cinnamates, which cannot meet a reacting partner for dimerization, undergo the photo-isomerization reaction.

To determine the extent of the photo-reaction which includes photo-isomerization, photo-dimerization of the cinnamate group and photo-degradation of the polyimide main chain, the time dependent change of the absorbance at 284 nm with irradiation by polarized UV was investigated for PI-CIN9, PI-CIN32, and PI-CIN100, as shown in figure 8. The rapid decrease of the absorbance in the early stages of the irradiation, followed by a gradual decrease were observed for all the samples except for PI-CIN0. For PI-CIN0, the decrease in the absorbance becomes apparent after irradiation of 3 J cm^{-2}; this is associated purely with photo-degradation of the polyimide main chain. Considering the low photo-reactivity of the polyimide main chain, it is reasonable to regard the considerable decrease in the absorbance for PI-CIN9, PI-CIN32, and PI-CIN100 in the initial stages of irradiation as being due to photo-reaction of the cinnamate groups. The slow changes of the absorbances for PI-CIN9, PI-CIN32, and PI-CIN100 above 10 J cm^{-2} suggest that the photo-reaction of cinnamate groups becomes negligible and the gradual degradation of the polyimide main chain dominates the spectral changes.

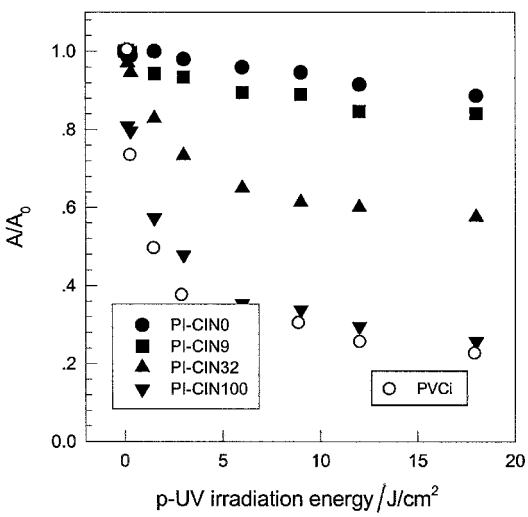

Figure 8. Change of absorbance at 284 nm with polarized UV irradiation in the UV spectra for PI-CINs.

It should be stressed here that for PI-CIN100, there was a decrease of about 80% in the initial absorbance at 284 nm upon polarized UV irradiation. Since the absorbance includes a contribution from the polyimide main chain, the decrease due to photo-reaction of the cinnamate group would be larger than 80%. It is quite comparable to that for PVCi: PVCi showed about an

80% decrease in the initial absorbance after prolonged polarized UV irradiation (see figure 8). In spite of the large difference in chain rigidity between PI-CIN100 and PVCi, the extent of the photo-reaction of pendant cinnamate groups was not much different. The aggregation of cinnamate groups bound to polyimide, which increases the probability of two cinnamate groups meeting, can be expected for PI-CIN100, as previously suggested for PVCi [32].

The generation of the structural anisotropy of the thin PI-CIN layers by polarized UV irradiation is important with regard to homogeneous LC alignment. Figure 9 shows the polarized UV spectra for the polarized UV exposed PI-CIN thin films. Generation of dichroism in the cinnamate absorption at around 284 nm by the exposure to polarized UV is apparent irrespective of the cinnamate content. The cinnamate absorption for polarization direction of the probing UV radiation parallel to that of the actinic UV was found to be less than that for the perpendicular case. It is due to the higher degree of photo-reaction of the cinnamate groups aligned along the polarization direction of the actinic UV. For quantitative comparison of the structural dichroism, the dichroic ratio (DR), defined as $DR = (A_\perp - A_\parallel)/(A_\perp + A_\parallel)$, was determined. Here $A_\perp$ and $A_\parallel$ are the absorbances at 278 nm of the cinnamates with probing light of electric vectors perpendicular to and parallel with, respectively, an electric vector of the actinic polarized light.

Figure 10 shows the time-dependent changes of the DR during the irradiation with polarized UV (5 mW cm^{-2}) for PI-CIN9, PI-CIN32, and PI-CIN100. For all the samples, an abrupt increase in the dichroism was observed at an early stage in the polarized UV irradiation, followed by a decrease and final saturation in DR upon prolonged irradiation. The eventual DR values showed the following order: PI-CIN9 < PI-CIN32 < PI-CIN100. The rapid increase in DR value in the early stages of the polarized UV irradiation indicates that a cinnamate group parallel to the UV polarization reacts more rapidly due to the higher probability of UV absorption in the early stages. The decrease in the difference in DR value after reaching a certain maximum is possibly explained as follows. The rate of reaction of cinnamate groups oriented along the direction of the UV polarization will decrease due to depletion of reacting sites in this direction, and so the reaction rate of the cinnamate groups oriented perpendicularly to the UV polarization becomes closer to that of the cinnamate group having the parallel orientation, causing the diminution in DR.

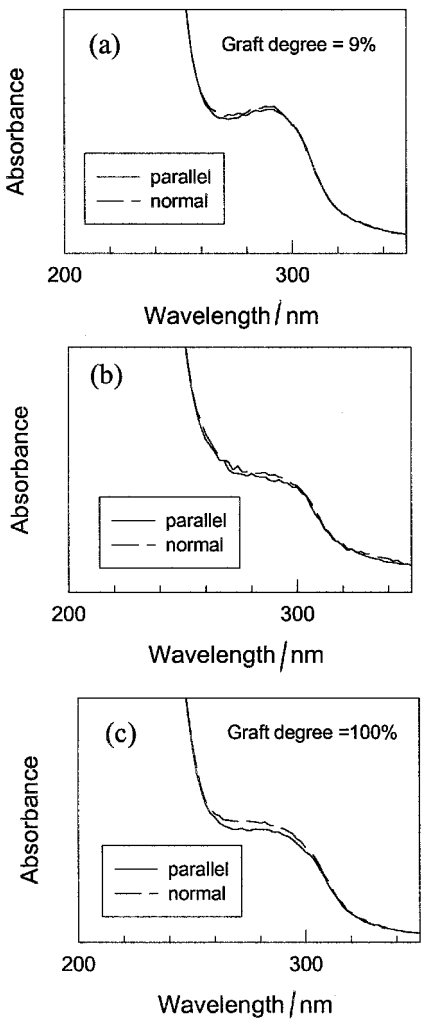

Figure 9. Polarized UV spectra for (*a*) PI-CIN9, (*b*) PI-CIN32, (*c*) PI-CIN100.

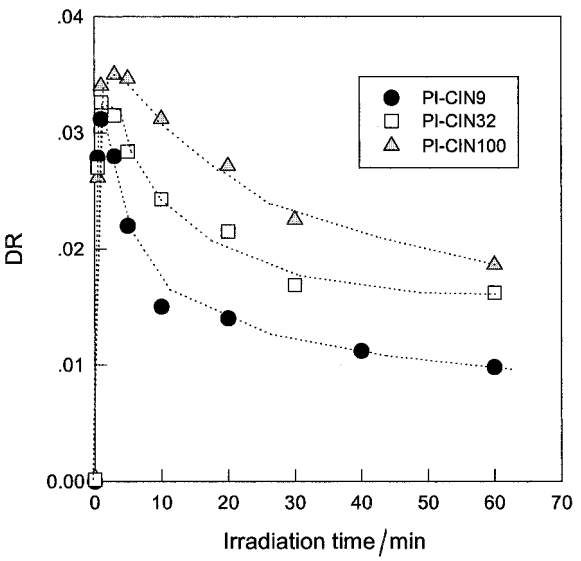

Figure 10. Plot of dichroic ratio as a function of irradiation time with polarized UV for PI-CIN9, PI-CIN32 and PI-CIN100.

Downloaded At: 18:24 25 January 2011

3.6. *Effect of cinnamate content on the photo-induced liquid crystal alignment*

In order to examine the characteristics of the photo-induced LC alignment on the thin layer of PI-CIN, parallel LC cells with PI-CIN alignment layers were prepared. The irradiation energy for the preparation of the alignment layers was 3 J cm^{-2}. Figure 11 displays the polarizing optical microscope images of the LC cells prepared with alignment layers based on PI-CINs. For the cinnamate-containing polyimides, dark and bright images appeared successively on rotating the LC cells between crossed polarizers. This behaviour is characteristic of the homogeneous alignment of a nematic LC. The high contrast beween the dark and bright images indicates that the liquid crystal alignments given by the PI-CIN alignment layers were quite uniform. However, PI-CIN0 did not show homogeneous liquid crystal alignment, even though the polyimide itself is known to align a liquid crystal through exposure to polarized UV. Even in the case of high energy irradiation of 9 J cm^{-2}, LC alignment was found to be poor. This seems to be associated with the low photo-reactivity of the imide segment and the flexibility of the alkyl chain, which may randomize the anisotropic distribution of the photo-cleaved residue. From the fact that PI-CIN0 does not efficiently induce homogeneous LC alignment by polarized UV irradiation, it can be concluded that homogeneous LC alignment by the PI-CIN layer is predominantly generated from structural anisotropy induced by the photo-reaction of the pendant cinnamate group.

The alignment direction of the nematic liquid crystal on the PI-CIN alignment layer was determined from the anisotropic absorption of a small amount of dichroic dye (disperse blue 14) dissolved in the liquid crystal layer. The dichroic dye shows strong absorption at 656 nm, and from the angular dependence of the absorbance at 656 nm in the polarized UV spectra of the LC cell, as shown in figure 12, the distribution of the LC director can be obtained. It is found that the PI-CIN alignment layers align the LC perpendicular to the polarization direction of the UV irrespective of the cinnamate content, as does the pure PVCi alignment layer.

In order to quantify how effectively the PI-CIN alignment layers align the LC unidirectionally, we measured the azimuthal anchoring energy of the LC on the PI-CIN alignment layers. A high azimuthal anchoring energy is indicative of a strong anisotropic interaction between alignment layer and LC, and figure 13 compares the azimuthal anchoring energy of the nematic LC (E7) on thin layers based on PI-CIN9, PI-CIN32, and PI-CIN100. Interestingly, they give almost the same

Downloaded At: 18:24 25 January 2011

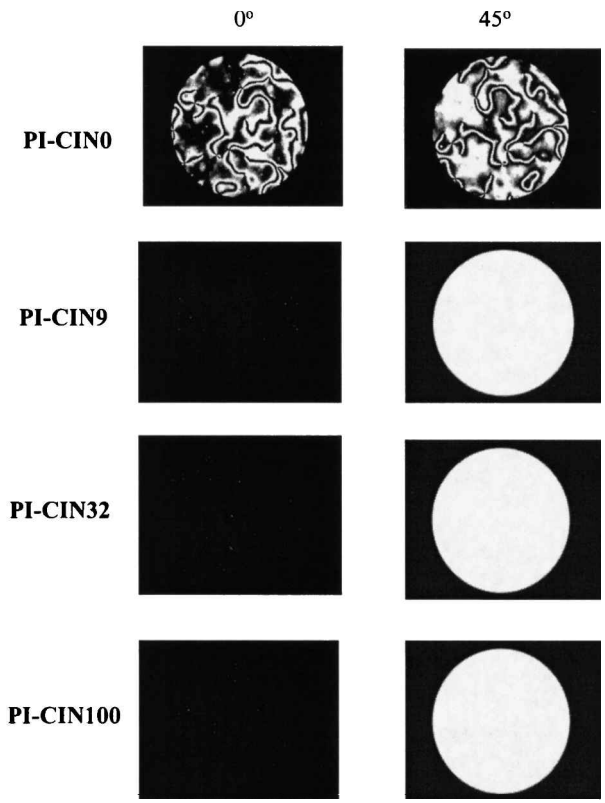

Figure 11. Polarized optical microscopy images of parallel aligned LC cells based on PI-CIN0, PI-CIN9, PI-CIN32 and PI-CIN100.

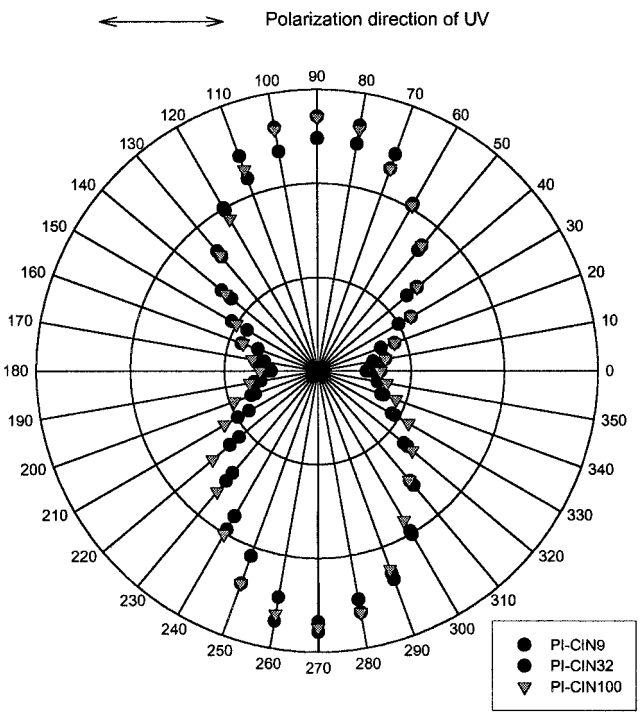

Figure 12. Polar plot of the absorbance of dichroic dye dissolved in the LC in the cells based on PI-CIN9, PI-CIN32 and PI-CIN100.

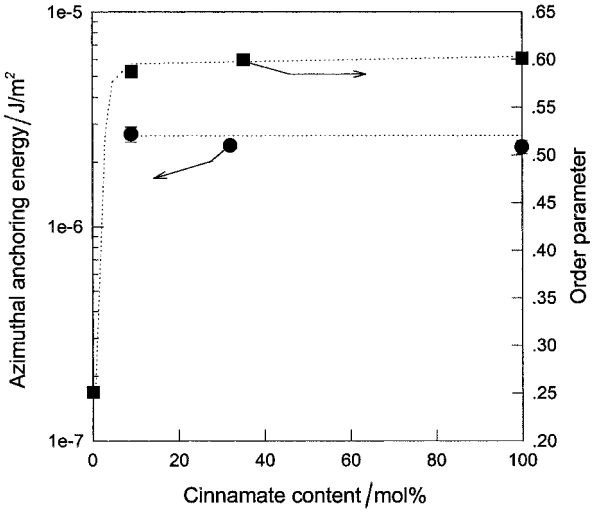

Figure 13. Azimuthal anchoring energy and order parameter of the LC as a function of the cinnamate content.

value of the azimuthal anchoring energy in spite of the difference in the *DR* value. The maximum anchoring energy obtained for the PI-CINs was 3.1×10^{-6} J m^{-2} which is comparable to that for PVCi (4×10^{-6} J m^{-2}) [7, 22]. A consideration of the surface structure provides a feasible explanation for this behaviour. Due to the preferential occupation of the surface of the PI-CIN thin layer by the cinnamate group, the structural dichroism of the surface may be less influenced by the cinnamate content than that of the bulk layer.

In addition to the azimuthal anchoring energy, the order parameter of the nematic LC was measured. As shown in figure 13, the order parameter of the LC is not dependent on the cinnamate content. The similarity in the cinnamate content dependences between the azimuthal anchoring energy and the order parameter implies that the degree of uniformity of the LC alignment in the LC layer is dictated by the strength of the surface anchoring of the LC on the alignment layer.

3.7. *Mechanism of the photo-induced LC alignment on PI-CIN thin layers*

According to Schadt *et al.* [4], the surface-settled homogeneous alignment of a nematic LC results from the linearly polarized light-induced photo-dimerization of the cinnamate moieties in the PVCi thin film whereby cyclobutane ring systems are formed. On the other hand, Ichimura *et al.* [14, 15] suggested that the photo-induced homogeneous LC alignment is caused by a polarization photochroism at the uppermost surface of the substrate, as a result of the repeated photo-isomerization of the cinnamate unit in PVCi. Since the photo-dimerization and the photo-isomerization could occur simultaneously, it is very hard to distinguish each contribution to the LC alignment. Recently, the contribution of photo-isomerization to LC alignment was removed by the hydrogenation of the undimerized cinnamate and the corresponding changes in the LC alignment for PVCi were reported [37]. The azimuthal anchoring energy was nearly unchanged by removal of the remaining cinnamate groups, which suggests that photo-dimerizati on can induce homogeneous LC alignment. However, this result cannot be absolute evidence for the absence of a contribution from the photo-isomer to LC alignment.

In order to identify the contribution of photo-isomerization to LC alignment for the PI-CIN alignment layers, we tried to remove the contribution from photo-dimerization. Our strategy was to irradiate the PI-CIN layers with unpolarized UV light to complete effectively any possible photo-dimerization. The photo-dimer produced by the irradiation by the unpolarized UV is isotropically distributed, and thus, it cannot induce homogeneous LC alignment, due to the absence of anisotropic interaction between the alignment layer and the LC. After a high dose of unpolarized UV, the layer was irradiated with polarized UV light. During this irradiation, the photo-isomerization of isolated cinnamate groups takes advantage from the photo-dimerization, because the remaining cinnamate groups cannot meet reacting partners for dimerization due to depletion of the neighbouring cinnamate groups by the first exposure to unpolarized UV. Therefore, the anisotropy developed during the second exposure to polarized UV is mainly attributed to the photo-isomerization of the remaining cinnamate groups. In this experiment, PI-CIN9 has merit because exclusive photo-isomerization occurs at a prolonged exposure higher than 6 J cm^{-2}, as indicated by the appearance of the isobestic point.

Figure 14 shows the distribution of the LC director for PI-CIN9 and PI-CIN100 thin layers which were successively exposed to unpolarized UV (32 J cm^{-2}) and to polarized UV (3 J cm^{-2}) radiation. Although the LCs aligned perpendicular to the polarization direction of the second exposure, the uniformities of the alignments were much lower than those of LC alignments induced by a single exposure to polarized UV (3 J cm^{-2}) as typically shown in figure 12. LC alignment by the single exposure includes contributions from both photo-dimerization and photo-isomerization. The above results indicate that photo-isomerization can contribute to uniform liquid crystal alignment to some extent, but that anchoring of the LC induced by anisotropic photo-isomerization is not as strong as that given by photo-dimerization.

3.8. *Thermal stability of the photo-induced liquid crystal alignment on PI-CIN thin layers*

As mentioned earlier, the structural design for PI-CIN layers was aimed at improving the thermal stability of

Downloaded At: 18:24 25 January 2011

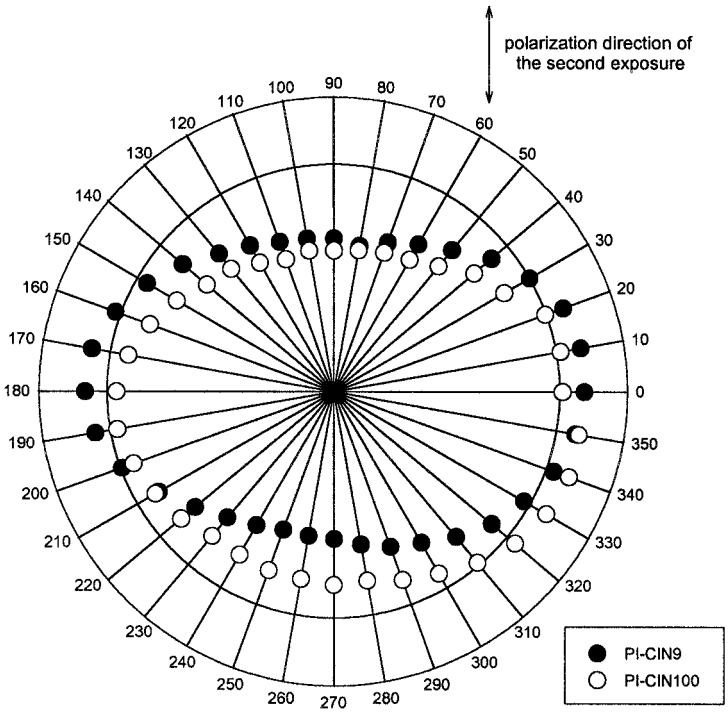

Figure 14. Polar plot of the absorbance of dichroic dye dissolved in LC in the cells based on PI-CIN9 and PI-CIN100 alignment layers prepared with a successive irradiation of 32 J cm^{-2} of unpolarized UV and 3 J cm^{-2} of polarized UV.

Downloaded At: 18:24 25 January 2011

photo-induced LC alignment. The thermal stability of the LC alignment on PI-CIN layers was evaluated by the following procedure. The PI-CIN layers exposed to polarized UV of 3 J cm^{-2} were annealed at various temperatures for 10 min and the azimuthal anchoring energies of the LC were measured for the homogeneously aligned LC cell prepared with annealed alignment layers.

Figure 15 shows the azimuthal anchoring energy of the LC as a function of the annealing temperature for PI-CIN9, PI-CIN32, PI-CIN100, and PVCi. The best thermal stability of the azimuthal anchoring of the photo-aligned LC was observed at the lowest cinnamate content. The azimuthal anchoring energies for PI-CIN32 and PI-CIN100 were gradually decreased by increase in the annealing temperature. However, the PI-CIN9 alignment layer gave a quite uniform LC alignment even after annealing at 200°C for 10 min.

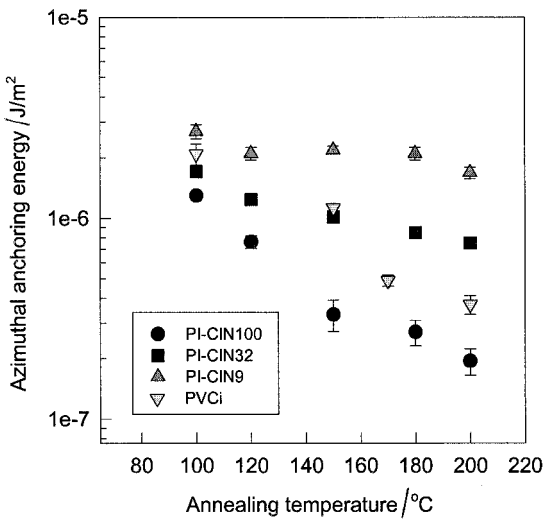

Figure 15. Azimuthal anchoring energies as a function of the annealing temperature of the PI-CIN alignment layers (annealing time: 10 min).

It should be stressed that the reduction in azimuthal anchoring energy takes place at temperatures much lower than the T_g of the alignment material. Although a further increase in the T_g of the alignment layer is expected after the UV irradiation, due to the formation of the crosslink, a significant lowering of the azimuthal anchoring energy occurs for PI-CIN32, and PI-CIN100 even at 120°C, which is much lower than the T_g of the materials. This indicates that not the long range motion of the chain, but the local disordering of the anchoring site, where the LC makes an effective anisotropic interaction, is responsible for the decrease in azimuthal anchoring energy. In that sense, the exceptional outstanding thermal stability of the LC alignment for PI-CIN9 could be attributed to a strong local anchoring of the main chains which effectively prevents local disordering of the photo-dimer.

On the other hand, comparison of the thermal stability of the photo-induced LC alignment between PI-CIN100 and PVCi leads to consideration of the effect of chain stiffness on the change of chain conformation during polarized UV irradiation. As compared in figure 15, PVCi showed a better thermal stability of the azimuthal

anchoring energy than PI-CIN100, in spite of its much lower T_g. This reconfirms that the thermal stability of the LC alignment is not related simply to the T_g of the material: T_g values of PI-CIN100 and PVCi are 183°C and 77°C, respectively.

A feasible explanation for this behaviour can be proposed in terms of the local stress near the photo-dimer developed during polarized UV irradiation. For a proper photo-dimerization, two cinnamate groups should collide to form the dimer involving positional and conformational changes of the chains near the cinnamate groups. In the case that local motion of the main chain is impossible, a significant local stress would be developed at the linkage of the cyclic dimer and the main chain, because of local displacement of the cinnamate groups and with a significant extension of the chain around the linkage. In contrast, when the main chain is flexible, photo-dimerization with local displacement of the main chain would be possible, effectively lowering local stress near the linkage. At an enhanced annealing temperature, dissipation of the stress by local displacement of the cyclic dimer may be favoured, resulting in a decrease in the anisotropic orientation of the dimer.

3.9. *Effect of photo-reaction temperature on the LC alignment*

In order to find evidence for the development of local stress in the PI-CIN100 alignment layer, the photo-reaction temperature dependence of photo-induced LC alignment was investigated. With increasing photo-reaction temperature, local motion of the main chain becomes easier and lowers the generation of local stress during photo-dimerization. However, increase in the photo-reaction temperature also induces long range diffusion of the chain, resulting in randomization of the anisotropic orientation of the dimer. Figure 16 shows the azimuthal anchoring energy as a function of the photo-reaction temperature. At 180°C, a maximum value for the azimuthal anchoring energy was observed, and further increase in the reaction temperature resulted in a large decrease in the azimuthal anchoring energy. The local mobility of the chain at 180°C is expected to give rise to an effective anisotropic photo-reaction. This result is in good agreement with the above considerations on the photo-reaction temperature dependence of the local stress and long-range diffusion of the chain.

Figure 17 compares the thermal stability of azimuthal anchoring of the LC for the two PI-CIN layers that were exposed to polarized UV of $3\,J\,cm^{-2}$ at room temperature and 180°C, respectively. The photo-reaction at 180°C showed better thermal stability of azimuthal anchoring of the LC than that conducted at room temperature. This strongly supports the view that the

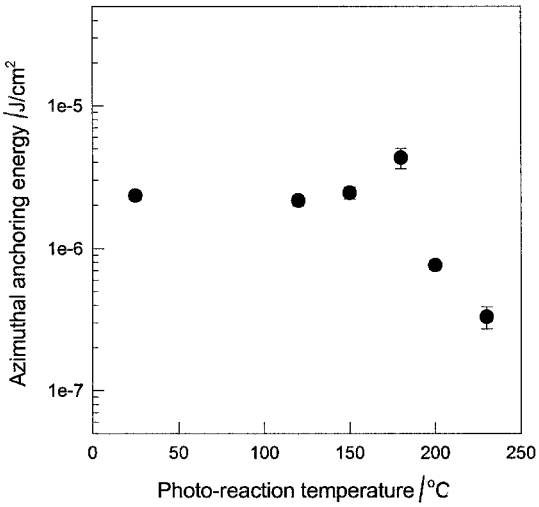

Figure 16. Azimuthal anchoring energy as a function of photo-reaction temperature for the PI-CIN100 alignment layer.

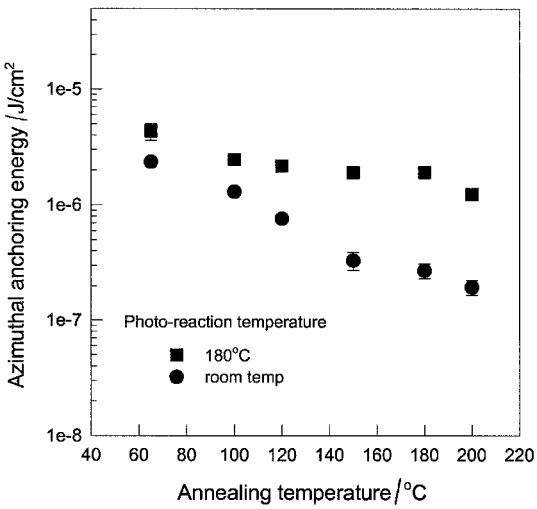

Figure 17. Comparison of the thermal stability of azimuthal anchoring between two PI-CIN100 alignment layers for which the photo-reaction temperatures were room temperature and 180°C.

generation of local stress during polarized UV irradiation significantly affects the reduction in thermal stability of the LC alignment.

Spectroscopic evidence for the development of local stress during dimer formation, the dissipation of the stress at an elevated annealing temperature, and the decrease in local stress at high photo-reaction temperatures were obtained by FTIR spectroscopy. The changes in molecular conformation due to local stress often result in a shift of the frequency of the maximum intensity of a band [38–41]. The alkyl chain of the main chain would be most profoundly deformed by local stress due to its flexibility. For that reason, the peak shape of the CH stretching vibration was investigated as a probe of the

Downloaded At: 18:24 25 January 2011

local stress. Figure 18 shows the CH stretching vibration for UV exposure PI-CIN100 thin layers which are different in photo-reaction temperature, as well as in annealing temperature, from the unexposed PI-CIN100 layers. After the polarized UV irradiation at room temperature, a new peak appeared at a lower wavenumber than that for normal CH stretching. However, this was not observed when the photo-reaction temperature was 180°C. The new peak at 2880 cm^{-1} could be assigned to CH stretch for the dimer in which a significant local stress exists. The peak at 2880 cm^{-1} disappeared after annealing at 150°C for 10 min, indicating dissipation of the residual stress by local rearrangement of the dimer. These spectroscopic results were in good agreement with the changes in LC alignment with photo-reaction temperature and annealing temperature. It should be mentioned that PVCi does not show any change in the CH stretching vibration after photo-reaction at room temperature, as shown in figure 19. The main chain flexibility of PVCi would provide a stable dimer without generating local stress, leading to better thermal stability of the LC alignment on PVCi compared with PI-CIN100.

3.10. *Pretilt angle of the nematic LC on PI-CIN layers*

The pretilt angle of a nematic LC, which is required for avoiding the occurrence of reverse tilt disclinations, was investigated for the PI-CIN alignment layers for various cinnamate contents and annealing temperature of the LC cell. In this work, the modified double exposure method which consists of exposure first to linearly polarized UV at normal incidence (3 J cm^{-2}) and second to unpolarized UV (1.2 J cm^{-2}) at an incidence angle of 45°, was used as described previously [42].

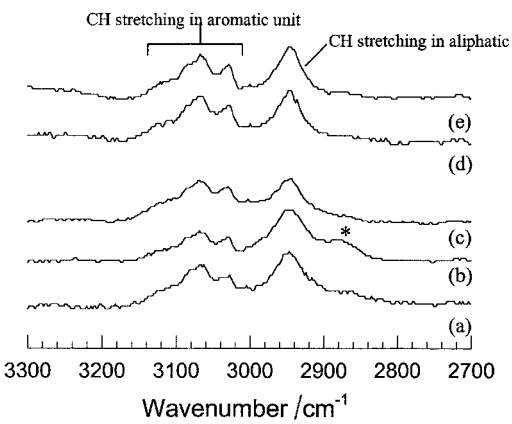

Figure 18. FTIR spectra of PI-CIN100 thin layers in the region 2700–3300 cm^{-1} (*a*) before p-UV irradiation, (*b*) after p-UV irradiation of 6 J cm^{-2} at room temperature, (*c*) after p-UV irradiation of 6 J cm^{-2} at 180°C, (*d*) after p-UV irradiation of 6 J cm^{-2} at room temperature and annealing at 150°C for 10 min, (*e*) after p-UV irradiation of 6 J cm^{-2} at 180°C and annealing at 150°C for 10 min.

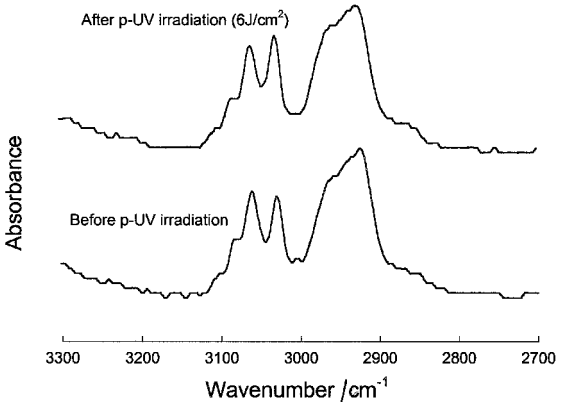

Figure 19. Comparison of FTIR spectra of PVCi thin layers in the region 2700–3300 cm^{-1} before and after p-UV irradiation of 6 J cm^{-2}.

Table 3 summarizes the results on pretilt angle. By using the modified double exposure method, we succeeded in creating a pretilt angle of about 1° for PI-CIN alignment layers. With increasing cinnamate content, the pretilt angle seems to be slightly increased. For PI-CIN32 and PI-CIN100, measurement of the pretilt angle after the annealing at 120°C was impossible due to significant disordering of the in-plane LC alignment. However, for PI-CIN9, it was found that the initial value of the pretilt angle was preserved, even after annealing at 120°C for 10 min. The stability of the pretilt angle increased in the order: PI-CIN100 < PI-CIN32 < PI-CIN9, as was the case for the azimuthal anchoring energy. The strong intermolecular interaction between the polyimide chains at low cinnamate content is therefore important to the thermal stability of the pretilt angle.

4. Conclusion

New polyimides with pendant cinnamate groups were synthesized and characterized. The cinnamate side groups were found to orient toward the surface, which makes it possible to induce good alignment irrespective of cinnamate content. The thermal stability of the photo-induced liquid crystal alignment was mainly influenced by the strong intermolecular interaction between imide segments, which impart a site for effective mobility restriction of the matrix. Stable alignment layers with a

Table 3. Pretilt angle (°) for PI-CIN9, PI-CIN32 and PI-CIN100.

Sample	65°C	100°C	120°C	150°C	180°C
PI-CIN9	0.81	0.75	0.73	0.23	0.05
PI-CIN32	0.93	0.81	0.25	—	—
PI-CIN100	1.08	0.53	—[a]	—	—

[a] The petilt angle cannot be determined due to significant disordering of the LC alignment.

Downloaded At: 18:24 25 January 2011

low local stress could be produced at an optimum photoreaction temperature, resulting in an increase in thermal stability of the LC crystal alignment.

This work was supported by the Center For Advanced Functional Polymers at KAIST in Korea.

References

[1] Gibbons, W., Shannon, P. J., Sun, S. T., and Swelin, B. J., 1991, *Nature*, **351,** 49.
[2] Iimura, Y., Kusano, J. I., Kobayashi, S., Aoyagi, Y., and Sugano, T., 1993, *Jpn. J. appl. Phys.*, **32,** L93.
[3] Ichimura, K., Akiyama, H., Kudo, K., Ishizuki, N., and Yamamura, S., 1996, *Liq. Cryst.*, **20,** 423.
[4] Schadt, M., Schmitt, K., Kozinkov, V., and Chigrinov, V., 1992, *Jpn. J. appl. Phys.*, **31,** 2155.
[5] Schadt, M., Seiberle, H., Schuster, A., and Kelly, S. M., 1995, *Jpn. J. appl. Phys.*, **34,** 3240.
[6] Schadt, M., Seiberle, H., Schuster, A., and Kelly, S. M., 1995, *Jpn. J. appl. Phys.*, **34,** L764.
[7] Bryan-Brown, G. P., and Sage, I. C., 1996, *Liq. Cryst.*, **20,** 825.
[8] Iimura, Y., Kobayashi, S., Hashimoto, T., Sugiyama, T., and Katoh, K., 1996, *IEICE Trans. Elect.*, **E79-C,** 1040.
[9] Schadt, M., Seiberle, H., and Schuster, A., 1996, *Nature*, **381,** 212.
[10] Kawatsuki, N., Takatsuka, H., Yamamoto, T., and Ono, H., 1997, *Jpn. J. appl. Phys.*, **36,** 6464.
[11] Chen, J., Johnson, D. L., Bos, P. J., Wang, X., and West, J. L., 1996, *Phys. Rev. E*, **54,** 2.
[12] Lu, J., Deshpande, S. V., Gulari, E., Kanicki, J., and Warren, W. L., 1996, *J. appl. Phys.*, **80,** 5028.
[13] Dyaduysha, A., Khizhnyak, A., Marusii, T., Reshetnyak, V., Reznikov, Y., and Park, W. S., 1995, *Jpn. J. appl. Phys.*, **34,** L1000.
[14] Ichimura, K., Akita, Y., Akiyama, H., Kudo, K., and Hayashi, Y., 1997, *Macromolecules*, **30,** 903.
[15] Ichimura, K., Akita, Y., Akiyama, H., Hayashi, Y., and Kudo, K., 1996, *Jpn. J. appl. Phys.*, **35,** L992.
[16] Jain, S. C., Rajesh, K., Samanta, S. B., and Narlikar, A. V., 1995, *Appl. Phys. Lett.*, **67,** 1527.
[17] Han, K. Y., Chae, B. H., Yu, S. H., and Song, J. K., 1997, *SID97 Dig.*, 707.
[18] Hwang, H., Lim, B., Chang, H., Kim, D., Kim, T., and Kim, Y., 1997, *Mol. Cryst. liq. Cryst.*, **295,** 89.
[19] Jang, Y. K., Yu, H. S., Yu, S. H., Song, J. K., Chae, B. H., and Han, K. Y., 1997, *SID97 Dig.*, 73.
[20] Song, S., Watabe, M., Adachi, T., Kobae, T., Chen, Y., Kawabata, M., Ishida, Y., Takahara, S., and Yamaoka, T., 1998, *Jpn. J. appl. Phys.*, **37,** 2620.
[21] Rajesh, K., Masuda, S., Yamaguchi, R., and Sata, S., 1997, *Jpn. J. appl. Phys.*, **36,** 4404.
[22] Kim, H. T., and Park, J. K., 1999, *Jpn. J. appl. Phys.*, **38,** 76.
[23] Li, X. T., Pei, D. H., Kobayashi, S., and Iimura, Y., 1997, *Jpn. J. appl. Phys.*, **36,** L432.
[24] Baur, G., Wittwer, V., and Berreman, D. W., 1976, *Phys. Rev. A*, **56,** 142.
[25] Han, K. Y., Miyashita, T., and Uchida, T., 1993, *Jpn. J. appl. Phys.*, **32,** L277.
[26] Kim, H. T., and Park, J. K., 1998, *Polym. Bull.*, **41,** 325.
[27] Ishida, H., Wellinghoff, S. T., Baer, E., and Koenig, J. L., 1980, *Macromolecules*, **13,** 725.
[28] Ishida, H., and Wuang, M. T., 1994, *J. polym. Sci. polym. Phys.*, **32,** 2271.
[29] Kim, H. T., and Park, J. K., 1997, *Polym. J.*, **29,** 1002.
[30] Kim, S. K., Kim, H. T., and Park, J. K., 1998, *Polym. J.*, **20,** 229.
[31] Kim, H. T., Kim, S. K., and Park, J. K., 1999, *Polym. J.*, **31,** 154.
[32] Egerton, P. L., Pitts, E., and Reiser, A., 1981, *Macromolecules*, **14,** 95.
[33] Egerton, P. L., Hyde, E. M., Trigg, J., Payne, A., Beynon, M., Mijovic, M. V., and Reiser, A., 1981, *J. Am. chem. Soc.*, **103,** 3859.
[34] Lin, A. A., and Reiser, A., 1989, *Macromolecules*, **22,** 3898.
[35] Rennert, J., 1971, *Photogr. Sci. Eng.*, **34,** 87.
[36] Paczkowski, J., Toczek, M., Scigalski, F., Cwiklinska, D., and Sierocka, M., 1989, *J. polym. Sci. polym. Chem.*, **27,** 2647.
[37] Kim, E. J., Park, O. O., Feng, L. H., Kawanami, Y., Furue, H., and Kobayashi, S., 1999, *Mol. Cryst. liq. Cryst.* (in the press).
[38] Bretzlaff, R. S., and Wool, R. P., 1983, *Macromolecules*, **16,** 1907.
[39] Koenig, J. L., 1992, *Spectroscopy of Polymers* (Washington DC: American Chemical Society), p. 26.
[40] Lee, Y. L., Bretzlaff, R. S., and Wool, R. P. J., 1984, *Polym. Sci. polym. Phys.*, **22,** 681.
[41] Wool, R. P., 1980, *Polym. Eng. Sci.*, **20,** 805.
[42] Kim, H. T., Lee, J. W., Sung, S. J., and Park, J. K., *Mol. Cryst. liq. Cryst.* (to be published).

Downloaded At: 18:24 25 January 2011